

Supporting Information

What is the initiation step of the Grubbs-Hoveyda olefin metathesis catalyst?

Ian W. Ashworth, Ian H. Hillier, David J. Nelson, Jonathan M. Percy and Mark A. Vincent

Contents

Page S2: Strategy for location of transition structures.

Page S3: Transition structures for dissociative, associative and interchange mechanisms.

Page S11: Full Gaussian03 reference.

Page S12: Experimental details and results.

Strategy for the location of Transition Structures.

The location of energy minima is usually quite routine using the powerful algorithms in Gaussian, which allow starting structures far from the final minimum to be used. However, the location of transition structures requires somewhat better starting structures, particularly when the energy surfaces are flat. We found this to be particularly true in the case of the interchange mechanism, central to the present study. Here, the energy surface associated with the approach of ethene to the ruthenium was explored manually to locate a starting structure having low energy gradients, but which corresponded to a local energy maximum. This structure was then refined using the algorithms in Gaussian.

Coordinates (Å)

Dissociative mechanism (Fig. 1 (a))

1	44	0	-2.548413	-1.863109	3.992229
2	6	0	-4.156337	-0.806411	3.924505
3	7	0	-4.575881	0.149853	3.041291
4	6	0	-5.704420	0.921644	3.572295
5	6	0	-6.219534	0.029161	4.685050
6	7	0	-5.058059	-0.818915	4.950467
7	1	0	-6.511500	0.578714	5.584052
8	1	0	-7.075257	-0.584046	4.367498
9	1	0	-6.442397	1.117880	2.789616
10	1	0	-5.345848	1.891685	3.944988
11	17	0	-3.159028	-4.093634	3.817291
12	17	0	-1.608428	-0.416763	5.550751
13	6	0	-5.123796	-1.850275	5.941169
14	6	0	-5.705009	-3.085238	5.601840
15	6	0	-5.729790	-4.084403	6.566651
16	6	0	-5.213510	-3.885323	7.847652
17	6	0	-4.704310	-2.631414	8.166889
18	6	0	-4.661064	-1.589817	7.237508
19	6	0	-4.187247	-0.235211	7.664731
20	1	0	-4.020402	0.431557	6.819580
21	1	0	-4.921796	0.227136	8.334480
22	1	0	-3.245701	-0.302570	8.214120
23	1	0	-4.327419	-2.449419	9.170999
24	6	0	-5.203537	-5.002779	8.844993
25	1	0	-4.434343	-5.741293	8.596517
26	1	0	-6.157992	-5.535884	8.863550
27	1	0	-4.996743	-4.642801	9.854649
28	1	0	-6.148487	-5.053566	6.304552

29	6	0	-6.322035	-3.321803	4.257085
30	1	0	-5.784720	-2.811406	3.456321
31	1	0	-6.327926	-4.385171	4.014455
32	1	0	-7.362792	-2.974903	4.238169
33	6	0	-3.981555	0.595340	1.822155
34	6	0	-4.562750	0.144065	0.624449
35	6	0	-4.023083	0.577564	-0.580284
36	6	0	-2.926978	1.443722	-0.622743
37	6	0	-2.382156	1.874356	0.581674
38	6	0	-2.888363	1.466686	1.819600
39	6	0	-2.207868	1.895603	3.078699
40	1	0	-1.387742	1.206755	3.311814
41	1	0	-1.787388	2.899383	2.977193
42	1	0	-2.864287	1.877222	3.950774
43	6	0	-5.680686	-0.852817	0.655153
44	1	0	-5.351636	-1.796852	1.104863
45	1	0	-6.534842	-0.511482	1.249079
46	1	0	-6.041822	-1.071051	-0.351129
47	1	0	-4.458133	0.220171	-1.511196
48	1	0	-1.524460	2.543796	0.567019
49	6	0	-2.360401	1.888318	-1.936063
50	1	0	-2.068784	1.033217	-2.552770
51	1	0	-1.479327	2.518303	-1.802774
52	1	0	-3.093232	2.458949	-2.515112
53	6	0	-2.015026	-1.587807	2.264496
54	1	0	-2.817498	-1.451594	1.531904
55	6	0	-0.745620	-1.882549	1.616093
56	6	0	-0.806365	-2.654642	0.442671
57	6	0	0.331068	-3.028452	-0.251772
58	6	0	1.570916	-2.595132	0.205904
59	6	0	1.667277	-1.792036	1.334806
60	6	0	0.522925	-1.429358	2.051954

61	1	0	2.642232	-1.445879	1.653915
62	1	0	2.476327	-2.868600	-0.326789
63	1	0	0.253450	-3.643043	-1.141632
64	1	0	-1.786506	-2.975926	0.099383
65	8	0	0.533251	-0.631948	3.143198
66	6	0	1.707983	0.160859	3.426776
67	1	0	2.584934	-0.501277	3.415412
68	6	0	1.521722	0.708761	4.820597
69	1	0	0.650413	1.366698	4.864588
70	1	0	1.362043	-0.092823	5.541996
71	1	0	2.405541	1.280942	5.113593
72	6	0	1.855864	1.254096	2.385772
73	1	0	0.989517	1.921259	2.421123
74	1	0	1.933354	0.850508	1.374015
75	1	0	2.750590	1.850047	2.582137

Associative mechanism (Fig. 1 (b))

1	6	0	1.109253	-3.293749	-0.870124
2	6	0	2.016419	-2.235708	-0.634626
3	6	0	3.392937	-2.494431	-0.741606
4	6	0	3.861200	-3.750240	-1.090909
5	6	0	2.949454	-4.782405	-1.292922
6	6	0	1.578046	-4.570111	-1.169701
7	6	0	1.518322	-0.947736	-0.227050
8	44	0	-0.293741	-0.595919	-0.110809
9	17	0	-2.347078	-1.183036	1.172931
10	8	0	-0.195636	-2.938642	-0.719611
11	6	0	-1.244945	-3.943086	-0.956982
12	6	0	-1.537461	-4.640410	0.352529
13	6	0	-0.264589	1.396315	-0.002614
14	7	0	-1.368012	2.174037	-0.215293
15	6	0	-1.061445	3.602010	-0.353866

16	6	0	0.393733	3.677766	0.055077
17	7	0	0.787512	2.266359	0.101810
18	6	0	-2.756137	1.832064	-0.120769
19	6	0	-3.329579	1.798881	1.161516
20	6	0	-4.683755	1.525828	1.274608
21	6	0	-5.480359	1.297734	0.150646
22	6	0	-4.895014	1.409738	-1.103859
23	6	0	-3.537797	1.703043	-1.270640
24	6	0	-2.486407	2.030469	2.374919
25	6	0	-3.006424	1.936896	-2.651377
26	6	0	-6.928220	0.946367	0.304343
27	6	0	2.180351	1.999196	0.214592
28	6	0	2.791218	2.072219	1.471148
29	6	0	4.155790	1.784827	1.557130
30	6	0	4.913350	1.474582	0.431419
31	6	0	4.282378	1.482475	-0.815196
32	6	0	2.922939	1.743806	-0.950502
33	6	0	2.026399	2.475974	2.696442
34	6	0	6.367835	1.133405	0.544065
35	6	0	2.254924	1.679745	-2.285951
36	17	0	-0.756097	-0.393050	-2.371014
37	6	0	-2.436927	-3.266519	-1.586735
38	6	0	0.526979	-1.964977	2.446383
39	6	0	0.609011	-0.654207	2.689930
40	1	0	3.303649	-5.778900	-1.537205
41	1	0	0.902232	-5.404911	-1.300481
42	1	0	4.082160	-1.676008	-0.545213
43	1	0	-2.171539	-2.818032	-2.543832
44	1	0	-3.208770	-4.022880	-1.756549
45	1	0	-2.849574	-2.491595	-0.938903
46	1	0	-1.723709	4.191182	0.287241
47	1	0	-1.234529	3.921419	-1.389779

48	1	0	0.540542	4.146160	1.037606
49	1	0	1.019661	4.215827	-0.663418
50	1	0	-0.826607	-4.645451	-1.684472
51	1	0	4.637116	1.811186	2.532493
52	1	0	4.864375	1.262883	-1.707988
53	1	0	-5.126719	1.466032	2.266138
54	1	0	-5.510507	1.280190	-1.991882
55	1	0	1.543516	2.498516	-2.433334
56	1	0	2.987492	1.712588	-3.094266
57	1	0	1.669957	0.759089	-2.390786
58	1	0	2.415868	1.983623	3.590592
59	1	0	2.112543	3.555054	2.869356
60	1	0	0.962162	2.243518	2.617447
61	1	0	-1.720651	1.253970	2.460845
62	1	0	-1.970052	2.997991	2.342244
63	1	0	-3.089635	2.004583	3.283718
64	1	0	-1.934762	2.129943	-2.660263
65	1	0	-3.174294	1.068277	-3.292648
66	1	0	-3.521347	2.787004	-3.113056
67	1	0	6.971168	1.705495	-0.166098
68	1	0	6.753349	1.327004	1.546516
69	1	0	6.544051	0.075113	0.323549
70	1	0	-7.435029	1.617856	1.003364
71	1	0	-7.458750	0.988827	-0.648969
72	1	0	-7.045158	-0.067629	0.700497
73	1	0	4.925814	-3.934701	-1.184696
74	1	0	-2.232698	-5.468394	0.190180
75	1	0	-1.992858	-3.938462	1.054915
76	1	0	-0.624934	-5.046972	0.798623
77	1	0	2.291890	-0.326551	0.232764
78	1	0	-0.251274	-0.095481	3.044553
79	1	0	-0.406601	-2.503104	2.567802

80	1	0	1.391707	-2.537700	2.120963
81	1	0	1.545749	-0.116769	2.579276

Interchange mechanism (Fig. 1 (c))

1	6	0	-5.337961	-1.760197	7.902774
2	6	0	-5.372555	-0.367419	7.717288
3	6	0	-4.724651	0.506522	8.602433
4	6	0	-3.965619	-0.048404	9.630495
5	6	0	-3.827103	-1.423881	9.785092
6	6	0	-4.533221	-2.262216	8.922400
7	7	0	-6.212252	0.179892	6.697935
8	6	0	-5.936842	0.252005	5.361338
9	7	0	-7.115985	0.595625	4.748682
10	6	0	-8.161029	0.940573	5.719186
11	6	0	-7.636335	0.326861	6.996570
12	44	0	-4.149859	0.083309	4.632845
13	17	0	-3.866688	-2.260854	4.859271
14	6	0	-7.450731	0.801668	3.375277
15	6	0	-8.162452	-0.227459	2.735966
16	6	0	-8.595438	-0.026110	1.429716
17	6	0	-8.333531	1.163601	0.747887
18	6	0	-7.623695	2.160237	1.411558
19	6	0	-7.177290	2.011314	2.725792
20	6	0	-8.368838	-1.541579	3.424768
21	6	0	-8.797503	1.365517	-0.662073
22	6	0	-6.385943	3.098850	3.376143
23	6	0	-4.812522	1.993725	8.469190
24	6	0	-2.909678	-1.982360	10.828364
25	6	0	-6.186822	-2.691984	7.092732
26	6	0	-4.764259	-0.142291	2.914048
27	6	0	-4.236878	0.200756	1.617784
28	6	0	-5.015843	-0.143565	0.494750

29	6	0	-4.665741	0.233913	-0.788178
30	6	0	-3.505726	0.979634	-0.974260
31	6	0	-2.698516	1.325467	0.103326
32	6	0	-3.036171	0.921982	1.398184
33	8	0	-2.278153	1.152069	2.489207
34	6	0	-1.212418	2.136677	2.393729
35	6	0	-0.339491	1.930953	3.603365
36	17	0	-3.625789	2.311493	5.250182
37	6	0	-1.804939	3.528772	2.319519
38	6	0	-1.828977	-0.326039	7.004989
39	6	0	-1.069459	-0.565145	5.929663
40	1	0	-3.215534	1.298140	-1.970811
41	1	0	-1.800940	1.901813	-0.077565
41	1	0	-1.800940	1.901813	-0.077565
42	1	0	-5.930489	-0.703159	0.671692
43	1	0	0.088281	0.927056	3.610259
44	1	0	0.477917	2.656385	3.598521
45	1	0	-0.929878	2.067631	4.511832
46	1	0	-7.781427	0.956974	7.878364
47	1	0	-8.080011	-0.657106	7.205333
48	1	0	-8.254754	2.033946	5.785198
49	1	0	-9.128889	0.542095	5.403458
50	1	0	-0.629891	1.911804	1.490612
51	1	0	-7.399455	3.088819	0.890101
52	1	0	-9.134003	-0.824531	0.924115
53	1	0	-3.432033	0.621003	10.301647
54	1	0	-4.463697	-3.340153	9.049911
55	1	0	-8.905073	-1.441187	4.374499
56	1	0	-8.933418	-2.232570	2.796742
57	1	0	-7.408333	-2.013284	3.666671
58	1	0	-6.759975	4.084201	3.087293
59	1	0	-6.381483	3.026738	4.464890

60	1	0	-5.333628	3.044173	3.074873
61	1	0	-5.594693	2.307594	7.776350
62	1	0	-4.989606	2.459670	9.442739
63	1	0	-3.875254	2.392694	8.072882
64	1	0	-6.411144	-2.300828	6.100000
65	1	0	-5.689791	-3.652956	6.953193
66	1	0	-7.135735	-2.887877	7.608631
67	1	0	-9.641111	2.062237	-0.709168
68	1	0	-8.005300	1.788061	-1.286378
69	1	0	-9.124069	0.428787	-1.118374
70	1	0	-2.981167	-1.430584	11.769189
71	1	0	-3.116389	-3.034514	11.033353
72	1	0	-1.866860	-1.912392	10.498458
73	1	0	-5.288604	-0.040670	-1.632504
74	1	0	-1.009192	4.271228	2.218463
75	1	0	-2.368181	3.739113	3.232104
76	1	0	-2.477064	3.638089	1.465075
77	1	0	-5.678735	-0.735092	2.804904
78	1	0	-2.672209	-0.964392	7.265414
79	8	0	-1.687577	0.666560	7.906742
80	1	0	-0.208280	0.036288	5.674495
81	1	0	-1.300333	-1.420793	5.309923
82	6	0	-0.665118	1.625070	7.650364
83	6	0	-0.721292	2.651655	8.749032
84	1	0	0.310760	1.119101	7.617058
85	1	0	-0.843360	2.075943	6.665198
86	1	0	0.060884	3.401558	8.614715
87	1	0	-1.685815	3.164568	8.751940
88	1	0	-0.581240	2.183933	9.726391

Full Gaussian 03 reference

M. J. Frisch, G. W. Trucks, H. B. Schlegel, G. E. Scuseria, M. A. Robb, J. R. Cheeseman, J. A. Montgomery, T. Vreven, K. N. Kudin, J. C. Burant, J. M. Millam, S. S. Iyengar, J. Tomasi, V. Barone, B. Mennucci, M. Cossi, G. Scalmani, N. Rega, G. A. Petersson, H. Nakatsuji, M. Hada, M. Ehara, K. Toyota, R. Fukuda, J. Hasegawa, M. Ishida, T. Nakajima, Y. Honda, O. Kitao, H. Nakai, M. Klene, X. Li, J. E. Knox, H. P. Hratchian, J. B. Cross, C. Adamo, J. Jaramillo, R. Gomperts, R. E. Stratmann, O. Yazyev, A. J. Austin, R. Cammi, C. Pomelli, J. W. Ochterski, P. Y. Ayala, K. Morokuma, G. A. Voth, P. Salvador, J. J. Dannenberg, V. G. Zakrzewski, S. Dapprich, A. D. Daniels, M. C. Strain, O. Farkas, D. K. Malick, A. D. Rabuck, K. Raghavachari, J. B. Foresman, J. V. Ortiz, Q. Cui, A. G. Baboul, S. Clifford, J. Cioslowski, B. B. Stefanov, G. Liu, A. Liashenko, P. Piskorz, I. Komaromi, R. L. Martin, D. J. Fox, T. Keith, M. A. Al-Laham, C. Y. Peng, A. Nanayakkara, M. Challacombe, P. M. W. Gill, B. Johnson, W. Chen, M. W. Wong, C. Gonzalez and J. A. Pople, *Gaussian 03, Revision D.02*, Gaussian Inc., Wallingford, CT, 2004.

Experimental

Dichloromethane was dried immediately before use using an Innovative Technologies PureSolv apparatus. Ethyl vinyl ether was purchased from Alfa Aesar and purified by distillation at atmospheric pressure on the day of use to remove stabilisers. Grubbs-Hoveyda 2nd generation pre-catalyst was purchased from Sigma-Aldrich and used as supplied. Stock solutions were prepared using dry volumetric glassware. Solvents and solutions were handled using dry glass syringes. The pre-catalyst and solutions thereof were handled with care under nitrogen at all times.

UV/Vis reaction mixtures were prepared as follows. A solution of ethyl vinyl ether in dichloromethane (typically 285 mg in 1 mL, *ca.* 4 mol L⁻¹) was accurately prepared. A concentrated stock solution of Grubbs-Hoveyda II was prepared (16.1 – 16.3 mM; 10.1 to 10.2 mg in 2 mL solvent) and diluted to approx. 0.3 mM in a 5 mL (185 μ L conc. stock) or 10 mL (370 μ L conc. stock) volumetric flask. An appropriate quantity of solvent (2.00, 2.00, 1.90 or 1.8 mL for 25, 50, 100 or 200 mM ethyl vinyl ether concentration, respectively) was accurately added to dry stoppered quartz cuvettes, followed by 1 mL of the dilute Grubbs-Hoveyda II stock.

UV/Vis spectra were recorded on a Cary 50 spectrometer equipped with a water-cooled peltier for temperature control. A baseline was recorded (using solvent dispensed at the same time as that used to prepare the samples in a clean cuvette) and then the reaction sample was equilibrated at the appropriate temperature in the spectrometer. An appropriate volume of ethyl vinyl ether solution (19 μ L = 25 mM, 38 μ L = 50 mM, 75 μ L = 100 mM, 150 μ L = 200 mM) was added, the cuvette was shaken, and UV spectra were recorded over time for 3 or more half-lives.

A sample UV/Vis spectrum can be found in **Figure S1**. The corresponding raw absorbance (abs.) *versus* time (t) dataset and processed dataset (**Figure S2**) are also provided in this document.

Absorbance/time data for $\lambda = 377$ nm was processed using the Guggenheim method (**Equation S1**) to obtain pseudo-first-order rate constants for each experiment (**Table S1**). Second order rate constants were calculated from the concentration and first-order rate constant (**Table S2**). These second order rate constants were used to construct a plot of

$\ln(k/T)$ versus $1/T$ (**Figure S3**), which was in turn used to derive the thermodynamic parameters for activation.

Figure S1. Sample UV/Vis spectra from the initiation of Grubbs-Hoveyda II (0.1 mM) with ethyl vinyl ether (200 mM) at 25°C in dichloromethane, showing well-behaved isosbestic points.

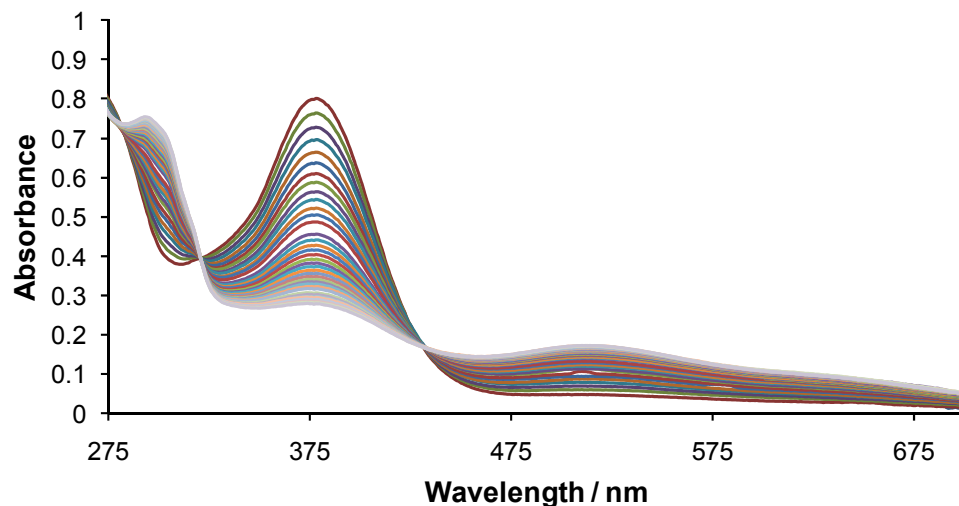
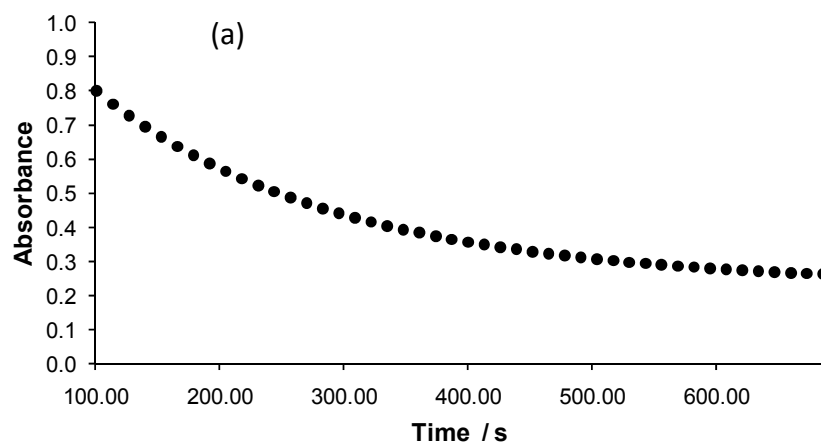
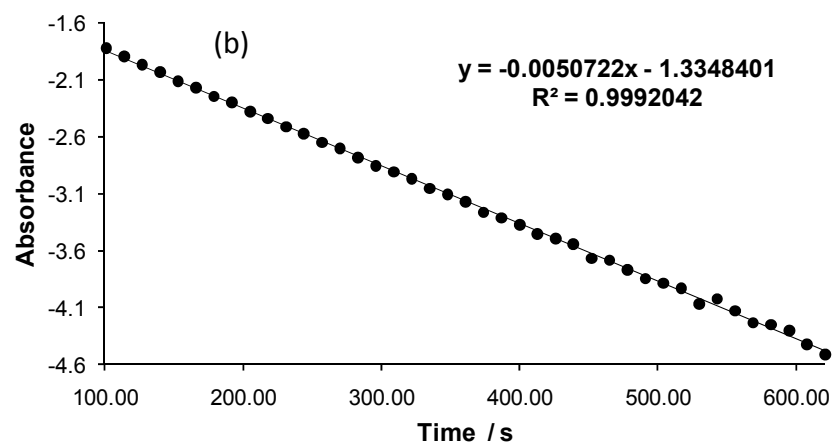


Figure S2. (a) Raw absorbance/time data and (b) data processed using the Guggenheim method ($k_{\text{obs}} = 5.072 \times 10^{-3} \text{ s}^{-1}$) for the reaction of Grubbs-Hoveyda II (0.1 mM) with ethyl vinyl ether (200 mM) at 25°C in dichloromethane.





Equation S1

$$\ln(\text{Abs}(t) - \text{Abs}(t+\Delta t)) = -k_{\text{obs}}t$$

Table S1. First-order rate constants. $R^2 > 0.997$ for all fits.

T (K)	[EVE] (mM)	k_{obs} (s^{-1})	T (K)	[EVE] (mM)	k_{obs} (s^{-1})
283.15	25.2	1.780×10^{-4}	283.15	24.8	1.815×10^{-4}
283.15	50.1	3.568×10^{-4}	283.15	49.3	3.640×10^{-4}
283.15	101.0	7.131×10^{-4}	283.15	99.3	7.039×10^{-4}
283.15	200.2	1.381×10^{-3}	283.15	197.0	1.380×10^{-3}
293.15	25.3	4.240×10^{-4}	293.15	25.0	4.192×10^{-4}
293.15	50.3	8.464×10^{-4}	293.15	49.6	8.304×10^{-4}
293.15	101.3	1.651×10^{-3}	293.15	100.1	1.677×10^{-3}
293.15	200.9	3.254×10^{-3}	293.15	198.4	3.205×10^{-3}
298.15	25.0	6.461×10^{-4}	298.15	24.8	6.559×10^{-4}
298.15	49.7	1.292×10^{-3}			
298.15	100.1	2.637×10^{-3}	298.15	99.5	2.624×10^{-3}
298.15	198.6	5.176×10^{-3}	298.15	197.3	5.221×10^{-3}
298.15	24.9	6.365×10^{-4}			
298.15	49.6	1.308×10^{-3}	298.15	50.0	1.292×10^{-3}
298.15	99.9	2.614×10^{-3}	298.15	100.8	2.625×10^{-3}
298.15	198.1	5.132×10^{-3}	298.15	199.8	5.090×10^{-3}
303.15	25.2	9.940×10^{-4}	303.15	24.9	9.818×10^{-4}
303.15	50.2	1.925×10^{-3}	303.15	49.5	1.960×10^{-3}
303.15	101.1	4.005×10^{-3}	303.15	99.8	3.821×10^{-3}
303.15	200.6	7.723×10^{-3}	303.15	198.0	7.461×10^{-3}

Table S2. Second-order rate constants. $R^2 > 0.999$ in all cases.

Temperature	k_{init}
283.15 K (1)	$0.00694 \text{ M}^{-1} \text{ s}^{-1}$
283.15 K (2)	$0.00704 \text{ M}^{-1} \text{ s}^{-1}$
293.15 K (1)	$0.01625 \text{ M}^{-1} \text{ s}^{-1}$
293.15 K (2)	$0.01630 \text{ M}^{-1} \text{ s}^{-1}$
298.15 K (1)	$0.02628 \text{ M}^{-1} \text{ s}^{-1}$
298.15 K (2)	$0.02634 \text{ M}^{-1} \text{ s}^{-1}$
298.15 K (3)	$0.02645 \text{ M}^{-1} \text{ s}^{-1}$
298.15 K (4)	$0.02611 \text{ M}^{-1} \text{ s}^{-1}$
303.15 K (1)	$0.03790 \text{ M}^{-1} \text{ s}^{-1}$
303.15 K (2)	$0.03871 \text{ M}^{-1} \text{ s}^{-1}$

Figure S3. Eyring plot for the initiation of Grubbs-Hoveyda II with ethyl vinyl ether in dichloromethane over the temperature range $10^\circ\text{C} - 30^\circ\text{C}$.

